

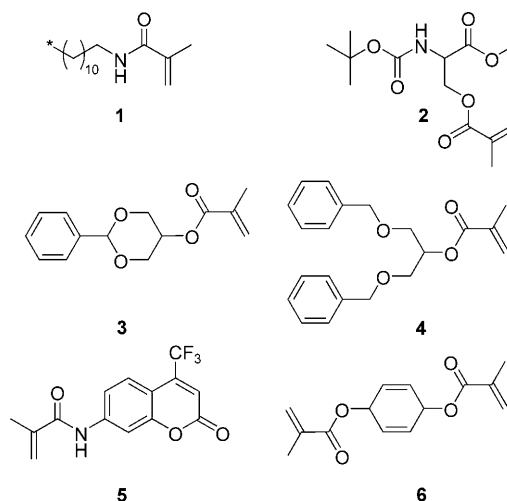
DOI: 10.1002/cmdc.201000250

## Ease of Synthesis, Controllable Sizes, and In Vivo Large-Animal-Lymph Migration of Polymeric Nanoparticles

Kimberly Ann V. Zubris,<sup>[a]</sup> Onkar V. Khullar,<sup>[c]</sup> Aaron P. Griset,<sup>[a]</sup> Summer Gibbs-Strauss,<sup>[b]</sup> John V. Frangioni,<sup>[b]</sup> Yolonda L. Colson,<sup>\*[c]</sup> and Mark W. Grinstaff<sup>\*[a]</sup>

Nanoparticles (NPs) are finding ever-increasing uses in a wide range of fields including photonics, catalysis and medicine, and identification of new compositions and synthetic methods is key to the continued discoveries with these materials. Within the medical arena, NPs are being investigated for drug delivery and medical imaging applications.<sup>[1–8]</sup> Our efforts are focused on exploring synthetic procedures that will enable a greater diversity of polymer compositions, encapsulants and sizes, and thus greater resultant NP utility. We recently reported the preparation of responsive NPs from an acrylate monomer for the triggered release of paclitaxel.<sup>[9]</sup> Here we further expand upon this synthetic approach and the use of two free-radical polymerization initiation methods. Both of these mild, room-temperature reactions allow for a range of monomers to be used and for control of particle size. As our interest lies in the diagnosis and treatment of lung cancer at its various stages, including metastases, we evaluated these NPs for lymphatic migration in a large animal.

NPs were prepared using a miniemulsion polymerization technique,<sup>[10–12]</sup> which combines high-energy emulsification and free-radical polymerization of an acrylate monomer and crosslinker. This is in contrast to the more common solvent evaporation method for synthesizing NPs (e.g., poly(lactic acid-glycolic acid) NPs),<sup>[13–19]</sup> which uses a previously synthesized polymer. Both photoinduced and base-catalyzed reactions were explored to initiate the free-radical polymerization. Specifically, NPs were prepared from monomers 1–5. The monomers were synthesized in good to high yields (59–88%) by reacting the primary hydroxy, secondary hydroxy or primary amine with methacryloyl chloride or methacrylic anhydride. The complete synthetic protocols can be found in the Supporting Information. These structures are representative of the diverse range of monomers that can be designed, synthesized



and used to prepare NPs with specific properties, including those monomers based on a carbohydrate (glycerol), an amino acid (serine), and a fluorescent dye (coumarin). This NP procedure is also amenable to working with a variety of common chemical linkages, such as esters, amides, ethers, carbamates and acetals, which are present in our monomers.

To prepare the NPs, the monomer (1–5) and a crosslinker (1,4-*O*-methacryloylhydroquinone, 6) were dissolved in a small amount of dichloromethane. The miniemulsion was formed by adding this organic solution to an aqueous solution of the surfactant sodium dodecyl sulfate (SDS) and sonicating the mixture under an argon blanket (Figure 1). Next, the free-radical-initiation system was added. When using the photochemical initiation method, eosin Y dye, 1-vinyl-2-pyrrolidinone, and triethanolamine were added to the emulsion, followed by irradiation under a xenon arc lamp. When using the base-catalyzed reaction, ammonium persulfate (APS) and *N,N,N',N'*-tetramethylethylenediamine (TEMED) were added to the emulsion while stirring under an argon blanket. Both initiation methods allow polymerization to be carried out under mild conditions at room temperature. The base-catalyzed initiation method also allows particles to be synthesized in the absence of light—critical when working with photosensitive monomers or encapsulants. Following polymerization using either method, the resultant NP suspensions were stirred overnight while open to the atmosphere to allow the remaining organic solvent to evaporate. The NPs were then dialyzed against phosphate buffer over two days to remove excess surfactant and salts. Dynamic light scattering (DLS) measurements revealed suspensions of relatively monodispersed, small-diameter NPs prepared from

[a] K. A. V. Zubris, Dr. A. P. Griset, Prof. M. W. Grinstaff  
Departments of Biomedical Engineering and Chemistry  
Metcalf Center for Science and Engineering, Boston University  
590 Commonwealth Avenue, Boston, MA 02215 (USA)  
Fax: (+1) 617-358-3186  
E-mail: mgrin@bu.edu

[b] Dr. S. Gibbs-Strauss, Dr. J. V. Frangioni  
Division of Hematology/Oncology, Department of Medicine  
Beth Israel Deaconess Medical Center, 330 Brookline Avenue, Boston, MA  
02215 (USA)

[c] Dr. O. V. Khullar, Dr. Y. L. Colson  
Division of Thoracic Surgery, Department of Surgery  
Brigham and Women's Hospital, 75 Francis Street, Boston, MA 02215 (USA)  
Fax: (+1) 617-730-2853  
E-mail: ycolson@partners.org

Supporting information for this article is available on the WWW under  
<http://dx.doi.org/10.1002/cmdc.201000250>.

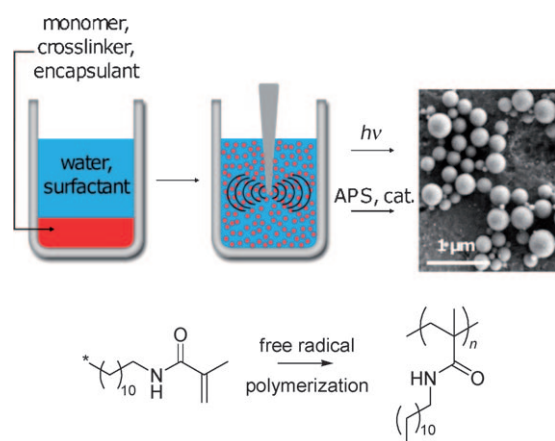


**Figure 1.** Schematic representation of NP synthesis. The organic monomer solution is emulsified in an aqueous surfactant solution using sonication, followed by free-radical polymerization.

monomers 1–4. Images obtained with scanning electron microscopy (SEM) show the spherical shape and smooth morphology of particles prepared with SDS (NPs composed of monomer 1 see Figure 1; NPs composed of monomers 2–4 see Figure 2). As shown in the micrographs, the size of the NPs was dependent upon which monomer was used.

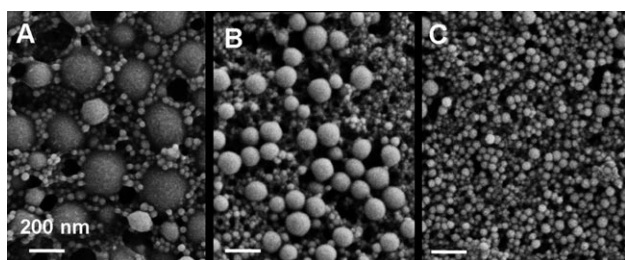


**Figure 2.** SEM micrographs of particles prepared from monomers 2–4, in panels A–C, respectively. Scale bar = 200 nm.

We also altered our experimental conditions to prepare NPs of various sizes. As shown in Table 1, the amount of SDS used when synthesizing NPs from monomer 1 was varied between 0.5 and 5 mg, thus enabling the synthesis of NPs with an average diameter as large as  $\approx 200$  nm and as small as  $\approx 50$  nm, respectively. Control of NP size depends not only on the particle composition, but also on the amount of surfactant present in the aqueous phase.

Next, pyrene was encapsulated within the NPs prepared from 1 as a model fluorescent molecular probe. Pyrene has an emission spectrum that contains five peaks. The relative intensities of the peaks I and III can be used to measure the local hydrophilicity/hydrophobicity of the pyrene environment.<sup>[20]</sup> Pyrene encapsulation was accomplished by adding pyrene (3% w/w monomer) into the organic solution of monomer while performing the miniemulsion polymerization procedure. The resulting particle suspension in water was excited at a wavelength of 321 nm, and the emission was recorded over

**Table 1.** Summary of the different sizes of NPs synthesized from monomer 1 as determined by DLS and SEM.

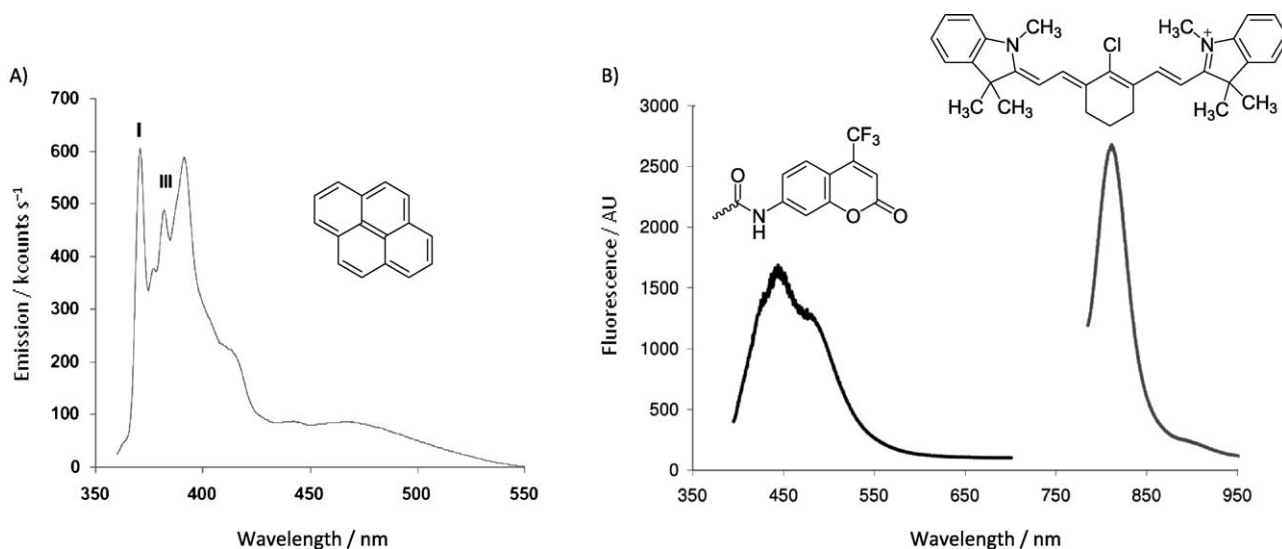
Entry	SDS [mg]	Diameter [nm]	
		via DLS	via SEM
1	0.5	215	182
2	2.5	134	110
3	5	61	40

Dynamic light scattering (DLS); nanoparticle (NP); scanning electron microscopy (SEM); sodium dodecyl sulfate (SDS).

the range of 360–550 nm. The encapsulated pyrene signal had a peak I/III ratio of 1.24, characteristic of a more hydrophobic medium than water, as the peak I/III ratio in water is 1.96.<sup>[20]</sup> This result confirmed entrapment of the dye within the hydrophobic NP (Figure 3).

The detection and subsequent treatment of lymph node metastases in patients is critically important for reducing morbidity and mortality.<sup>[21–23]</sup> Significant advances have been made in the detection of lymph node metastases using NPs. For example, superparamagnetic iron oxide NPs ( $\varnothing = 30$  nm) administered via intravenous injection will reach the lymphatic system and be transported to the lymph nodes in animals and patients. These lymph nodes can then be imaged using magnetic resonance imaging to determine the site of metastases.<sup>[24–26]</sup> There have also been reports describing the use of polymeric NPs, and this approach offers several opportunities for lymphatic imaging and drug delivery.<sup>[27–38]</sup> These previous studies were conducted using small-animal models (e.g., injection into a rat footpad or mouse tail), where the migration distances are limited. For our *in vivo* lymphatic migration studies, we synthesized NPs with a diameter of  $\approx 50$  and 120 nm from monomer 1 and the coumarin monomer 5 (5% w/w monomer of 1) loaded with the near-infrared (NIR) dye IR-786, using the base-catalyzed method. The emission spectrum of the resulting dual-labeled NPs is shown in Figure 3. Since the  $\lambda_{\text{max}}$  for emission is distinct for the two dyes, we were able to perform localization studies of the NP and encapsulant. Specifically, the NPs were injected subcutaneous into the breast of fully anesthetized Yorkshire pigs ( $n = 4$ ). The animals were imaged with a FLARE NIR imaging system 24 h later using a previously described method.<sup>[39]</sup> Migration was observed for the  $\approx 50$  nm NPs only. These NPs migrated over 20 cm to the regional draining lymph nodes within the neck or inguinal regions. As shown in Figure 4, the near-infrared, color-fluorescence-



**Figure 3.** A) Emission spectrum of NP-encapsulated pyrene (structure shown) with peaks I and III denoted. B) Emission spectra of NPs containing a covalently bound coumarin dye (—) and an encapsulated near infrared dye IR-786 (---). Dye structures are shown above their respective spectrum.

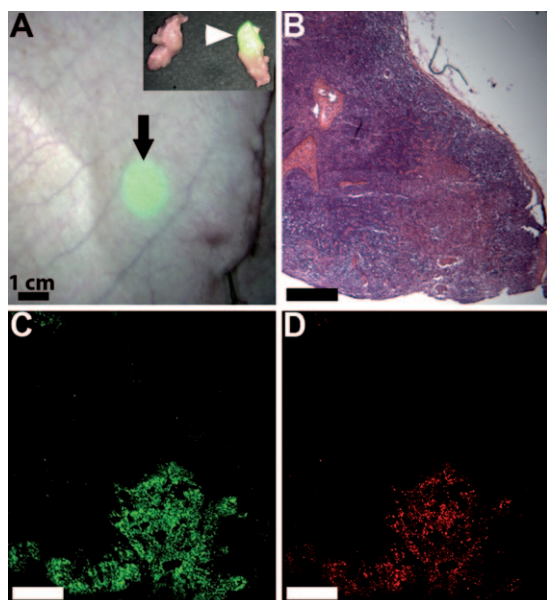


**Figure 4.** A) Visualization of the sentinel lymph node (arrow) through the skin of a live pig after injection of NPs loaded with IR-786 dye into the breast (not shown). Invisible NIR fluorescent light was pseudo-colored in lime green and superimposed on the color video image to produce this merged image. The NPs have localized in the lymph node 24 cm from the site of injection. The insert shows the fluorescent SLN after excision along with a nonfluorescent, negative adjacent node. B) Histological analysis of the lymph node confirms colocalization of C) encapsulated IR-786 and D) coumarin-labeled NP within the SLN.

merged image clearly shows delivery of the fluorescent NPs to the draining sentinel lymph node (SLN) from the injection site within the breast. Upon surgical removal of the sentinel lymph node and histological analysis with fluorescent microscopy,<sup>[40]</sup> we observed colocalization of the fluorescence signals of the coumarin and IR-786 dye within the SLN confirming delivery of the IR dye via the NP (Figure 4B–D). Our study demonstrates

that polymeric NPs are effective at migrating over large distances, which is critical for eventual human use.

In summary, we have synthesized polymeric NPs using a variety of monomers under mild conditions. This miniemulsion polymerization system allows different monomers and encapsulants to be easily combined, in addition to enabling the preparation of particles of different sizes. The room temperature, mild photoinduced or base-catalyzed polymerization methods also allow sensitive molecules, such as dyes, to be encapsulated. For example, NIR-dye-loaded NPs for lymphatic migration and lymph node localization were synthesized and successfully used in a large-animal model. Continued research in this area will increase our repertoire of materials and synthetic procedures available for the design of application-specific NPs. In the cancer arena, these investigations will facilitate the development of new approaches to identify nodal disease, characterize the extent of disease, and establish treatment regimes.

## Experimental Section

NPs were prepared using a miniemulsion polymerization method. Briefly, monomer **1**, **2**, **3**, **4** or **5** (50 mg) and crosslinker **6** (0.5 mg) were dissolved in CH<sub>2</sub>Cl<sub>2</sub> (0.5 mL). This solution was added to a 10 mM aq buffer solution (2 mL) containing 0.5–5 mg sodium dodecyl sulfate (SDS). This mixture was sonicated for 10 min (1 s pulses with a 2 s delay; 35 W) under an argon blanket to create the miniemulsion. When using the photochemical initiation method, following sonication, a 20 mM aq eosin Y solution (20 μL) and a 10% v/v aq 1-vinyl-2-pyrrolidinone solution (4.27 μL) were added to the emulsion. The mixture was then exposed to a xenon arc lamp (300 W) for 20 min while stirring to initiate polymerization. Alternatively, when using the base-catalyzed reaction, following sonication, a 200 mM aq ammonium persulfate (APS) solution (20 μL) and *N,N,N',N'*-tetramethylethylenediamine (TEMED) (2 μL) were added to the emulsion and stirred under an argon blanket for 2 h. Following polymerization using either method, the suspension was then stirred overnight while open to the atmos-

phere to allow the remaining solvent to evaporate. The resulting polymeric NPs were then dialyzed against 5 mM phosphate buffer (pH 8.0) over 2 d to remove excess surfactant and salts.

All animal experiments were conducted in accordance with the Beth Israel Deaconess Medical Center Institutional Animal Care and Use Committee (BIDMC IACUC)-approved protocol.

## Acknowledgements

This work was supported in part by funds from the Center for Integration of Medicine & Innovative Technology (MWG/YLC), Brigham and Women's Hospital (YLC), and the National Institutes of Health, grants R01-CA-115296 (JVF) and R01-EB-005805 (JVF).

**Keywords:** drug delivery · imaging agents · nanoparticles · polymerization · redox chemistry

- [1] V. P. Torchilin, *Adv. Drug Delivery Rev.* **2006**, *58*, 1532–1555.
- [2] M. E. Davis, Z. Chen, D. M. Shin, *Nat. Rev. Drug Discovery* **2008**, *7*, 771–782.
- [3] I. Brigger, C. Dubernet, P. Couvreur, *Adv. Drug Delivery Rev.* **2002**, *54*, 631–651.
- [4] K. Soppimath, *J. Controlled Release* **2001**, *70*, 1–20.
- [5] F. X. Gu, R. Karnik, A. Z. Wang, E. Levy-Nissenbaum, S. Hong, R. S. Langer, O. C. Farokhzad, *Nano Today* **2007**, *2*, 14–21.
- [6] P. Couvreur, C. Vauthier, *Pharm. Res.* **2006**, *23*, 1417–1450.
- [7] D. E. Owens III, N. A. Peppas, *Int. J. Pharm.* **2006**, *307*, 93–102.
- [8] L. Brannon-Peppas, J. O. Blanchette, *Adv. Drug Delivery Rev.* **2004**, *56*, 1649–1656.
- [9] A. P. Griset, J. Walpole, R. Liu, A. Gaffey, Y. L. Colson, M. W. Grinstaff, *J. Am. Chem. Soc.* **2009**, *131*, 2469–2471.
- [10] S. C. Thickett, R. G. Gilbert, *Polymer* **2007**, *48*, 6965–6991.
- [11] N. Anton, J. P. Benoit, P. Saulnier, *J. Controlled Release* **2008**, *128*, 185–199.
- [12] F. J. Schork, Y. Luo, W. Smulders, J. P. Russum, A. Butte, K. Fontenot, *Adv. Polym. Sci.* **2005**, *175*, 129–255.
- [13] R. A. Jain, *Biomaterials* **2000**, *21*, 2475–2490.
- [14] Y. Dong, S. S. Feng, *Int. J. Pharm.* **2007**, *342*, 208–214.
- [15] C. Fonseca, S. Simoes, R. Gaspar, *J. Controlled Release* **2002**, *83*, 273–286.
- [16] Y. Mo, L. Y. Lim, *J. Controlled Release* **2005**, *108*, 244–262.
- [17] J. Panyam, V. Labhasetwar, *Adv. Drug Delivery Rev.* **2003**, *55*, 329–347.
- [18] H. Sato, Y. M. Wang, I. Adachi, I. Horikoshi, *Biol. Pharm. Bull.* **1996**, *19*, 1596–1601.
- [19] D. V. Bazile, C. Ropert, P. Huve, T. Verrecchia, M. Marlard, A. Frydman, M. Veillard, G. Spenlehauer, *Biomaterials* **1992**, *13*, 1093–1102.
- [20] C. Tedeschi, H. Mothwald, S. Kirstein, *J. Am. Chem. Soc.* **2001**, *123*, 954–960.
- [21] G. Ravizzini, B. Turkbey, T. Barrett, H. Kobayashi, P. L. Choyke, *Wiley Interdiscip. Rev.: Nanomed. Nanobiotechnol.* **2009**, *1*, 610–623.
- [22] D. L. J. Thorek, A. Chen, J. Czupryna, A. Tsourkas, *Ann. Biomed. Eng.* **2006**, *34*, 23–38.
- [23] J. R. McCarthy, K. A. Kelly, E. Y. Sun, R. Weissleder, *Nanomedicine* **2007**, *2*, 153–167.
- [24] M. G. Harisinghani, J. Barentsz, P. F. Hahn, W. M. Deserno, S. Tabatabaei, C. H. van de Kaa, J. de La Rosette, R. Weissleder, *N. Engl. J. Med.* **2003**, *348*, 2491–U2495.
- [25] R. Weissleder, G. Elizondo, J. Wittenberg, A. S. Lee, L. Josephson, T. J. Brady, *Radiology* **1990**, *175*, 494–498.
- [26] A. G. Rockall, S. A. Sohaib, M. G. Harisinghani, S. A. Babar, N. Singh, A. R. Jeyarajah, D. H. Oram, I. J. Jacobs, I. J. Shepherd, R. H. Reznick, *J. Clin. Oncol.* **2004**, *23*, 2813–2821.
- [27] Y. Xie, T. R. Bagby, M. Cohen, M. L. Forrest, *Expert Opin. Drug Delivery* **2009**, *6*, 785–792.
- [28] J. Liu, D. Meisner, E. Kwong, X. Y. Wu, M. R. Johnston, *Cancer Res.* **2009**, *69*, 1174–1181.
- [29] D. A. Rao, M. L. Forrest, A. W. Alani, G. S. Kwon, J. R. Robinson, *J. Pharm. Sci.* **2010**, *99*, 2018–2031.
- [30] A. E. Hawley, L. Illum, S. S. Davis, *FEBS Lett.* **1997**, *400*, 319–323.
- [31] H. X. Lu, B. Li, Y. Kang, W. Jiang, Q. Huang, Q. H. Chen, L. M. Li, C. J. Xu, *Cancer Chemother. Pharmacol.* **2006**, *59*, 175–181.
- [32] P. Maincent, P. Thouvenot, C. Amicabile, M. Hoffman, J. Kreuter, P. Couvreur, J. P. Devissaguet, *Pharm. Res.* **1992**, *9*, 1534–1539.
- [33] V. Manolova, A. Flace, M. Bauer, K. Schwarz, P. Saudan, M. F. Bachmann, *Eur. J. Immunol.* **2008**, *38*, 1404–1413.
- [34] S. M. Moghimi, *FEBS Lett.* **2003**, *540*, 241–244.
- [35] S. M. Moghimi, A. E. Hawley, N. M. Christy, T. Gray, L. Illum, S. S. Davis, *FEBS Lett.* **1994**, *344*, 25–30.
- [36] S. T. Reddy, A. Rehor, H. G. Schmoekel, J. A. Hubbell, M. A. Swartz, *J. Controlled Release* **2006**, *112*, 26–34.
- [37] S. T. Reddy, A. J. van der Vlies, E. Simeoni, V. Angeli, G. J. Randolph, C. P. O'Neil, L. K. Lee, M. A. Swartz, J. A. Hubbell, *Nat. Biotechnol.* **2007**, *25*, 1159–1164.
- [38] Y. Nishioka, H. Yoshino, *Adv. Drug Delivery Rev.* **2001**, *47*, 55–64.
- [39] S. L. Troyan, V. Kianzad, S. L. Gibbs-Strauss, S. Gioux, A. Matsui, R. Oketokoun, L. Ngo, A. Khamene, F. Azar, J. V. Frangioni, *Ann. Surg. Oncol.* **2009**, *16*, 2943–2952.
- [40] A. Zaheer, R. E. Lenkinski, A. Mahmood, A. G. Jones, L. C. Cantley, J. V. Frangioni, *Nat. Biotechnol.* **2001**, *19*, 1148–1154.

Received: June 11, 2010

Published online on June 30, 2010